

## Bio-impedance signal decomposer: enhanced accuracy and reduced latency solution

Andrei Krivoshei

Tallinn University of Technology, Ehitajate tee 5, 19086 Tallinn, Estonia;  
andrei.krivoshei@elin.ttu.ee

Received 7 April 2011, in revised form 14 June 2011

**Abstract.** The paper presents an overview of the electrical bio-impedance (EBI) signal decomposition into its cardiac and respiratory components. This problem mainly originates from the non-stationarity of the signal components and overlapping of their harmonic spectra. In the introductory part of the paper, an overview of the bio-impedance signal decomposer (BISD), as a solution of the problem, is accompanied with an introduction to a cardiac BI signal model, which is constructed from the components of the application-specific orthonormal basis. In the main part of the paper a semi-synchronous cardiac signal amplitude estimator, which is based on the cardiac signal model and on the proposed extrema searching algorithm, is proposed. After that, the cardiac signal lock-in detection algorithm is proposed. Finally, a conditioning of the estimated cardiac signal frequency is discussed. The proposed amplitude estimator, lock-in detector and frequency conditioning increase twice the reaction speed of the BISD to the input EBI signal. The proposed version of the BISD estimates the cardiac signal amplitude during only a few cardiac periods, even if very large difference between amplitudes exists in different conditions. As a result, the entire BISD becomes locked during 8 s (including 4 s of soft start). The proposed improvements allowed reducing the latency of the BISD from 2 to 1 s.

**Key words:** bio-impedance, signal decomposition, heart rate monitoring, amplitude estimator, lock-in detector, model-based signal processing.

### 1. INTRODUCTION

It is well known that measurement of the electrical bio-impedance as a parameter of living tissue gives not only information about physiological performance of the tissue, but it also makes possible an analysis of the physiological processes or organs dynamics, such as respiration and heart activity.

The first correlation between the estimated EBI variations and the cardiac activity was published by Atzler and Lehmann [1] and by Nyboer et al. [2]. As a result, the term *impedance cardiography* (ICG) was introduced in 1959 [3,4].

The ICG is an EBI-based method that allows evaluating of hemodynamic parameters [5]. The time-variant part of the EBI, which is caused by cardiac activity, is taken as a basis for the ICG. The hemodynamic parameters, which are of the most interest for cardiologists, are the heart stroke volume (SV) and the cardiac output (CO).

Respectively, impedance respirography (IRG) is an EBI-based method allowing evaluation of pneumodynamic parameters. Consequently, the time-variant part of EBI, caused by breathing, is used as a basis for the IRG (also called impedance pneumography). The IRG can reflect the state of lungs and the respiratory system in general. The pneumodynamic parameters, especially minute ventilation (MV), reflect very closely the metabolic demand during physical exercises [6,7]. They can be used in rate-adaptive pacemakers [8-10] for estimation of the human workload by metabolic demand reflected in the impedance respirogram, and consequently, to adapt the heart pacing rate to an adequate value. The latter is possible due to the fact that the heart rate and the cardiac output are almost linearly related with MV [10].

However, direct analysis and extraction (estimation) of hemodynamic and pneumodynamic parameters from the EBI signal without decomposing it to the cardiac and respiratory components may be very complicated or impossible.

### 1.1. Publications overview

Over the past decades only tens of papers discuss the problem of EBI conditioning by separating its components, the cardiac and respiratory ones, in detail. The methods, discussed in these papers, can be divided into three parts: ensemble averaging, (classical) adaptive filtering, and spectral analysis methods. Trivial frequency domain filtering is not taken into account, because it is suitable only for some stationary conditions, i.e., for the healthy human in the resting state.

The ensemble-averaging is used in [11-13] to suppress disturbances in the first order time-derivative impedance cardiogram (DICGm). Woltjer et al. [14], referring to Kim et al. [15] declared that averaging has been shown to be effective in eliminating the effect of respiration. However, it is clear that the disturbing components must have a zero mean value to be effectively suppressed by averaging. But it becomes possible only, when averaging is done during a long time interval. Such averaging can suffer from the variability of the DICGm signal shape and event latencies that can cause less distinct events in the signal to disappear in the averaged signal [16].

Adaptive filtering is used by Yamamoto et al. [17] for suppression of the disturbances in the DICGm signal. This solution is based on the digital infinite impulse response (IIR) band-pass filter, which moves around the centre frequency (heart rate). Unfortunately, this solution can introduce non-linear phase distortion into the DICGm signal. Another application of the adaptive filtering for reducing the respiration and motion artefacts in electrogastrogram is described in [18]. Disadvantage of these filters appears in the need for a reference disturbance signal. The same disadvantage appears in a system for adaptive

cancellation of the respiratory artefact investigated in [19]. The scaled Fourier linear combiner (SFLC) [20] reconstructs the DICGm signal from harmonic spectral components, found by using an adaptive least mean square (LMS) filter, with reference inputs related to the R-R intervals of ECG.

The third approach is based on spectral analysis methods. In particular, the wavelet-based time-frequency analysis is used in [21,22] to select the disturbance-free DICGm signal from the noisy input. However, the spectral analysis, and using of wavelets in particular, require a great number of spectral components (levels in the wavelet case) to represent the input signal accurately. Another difficulty can arise by selection of the threshold, at which the separation of the useful component from noises is performed. In [22] the hard threshold is used, which has a disadvantage similar to the filtering with a constant cut-off frequency. The method [21] uses the soft threshold, but the breath holding during 8 s is needed to construct the auto-regressive (AR) model of the cardiac EBI signal. Moreover, the pre-whitening of the input EBI signal and spline-based model construction of the respiratory component are required.

In regard to the need of on-line, or even real-time, monitoring of the hemodynamic and pneumodynamic parameters during exercises and especially in the ambulatory conditions, the ensemble averaging approach is not suitable, because a long time interval is needed for collecting a great number of ICG periods, sufficient to perform an effective suppression of disturbances. The adaptive filtering and spectral analysis are more promising approaches despite the fact that some of these require a reference disturbance signal. Moreover, all the above described noise cancellation methods and systems require the heart rate estimates obtained from the electrocardiogram (ECG). The availability and accuracy of the ECG-based heart rate estimates are the mandatory prerequisites for the reliability of such methods. An exception to this rule is the coherent ensemble averaging method, investigated in [21]. However, although this method does not use the ECG signal, it has a common disadvantage with the ensemble-averaging technique.

Taking into account all mentioned above, it is clear that the decomposition of the total EBI signal into its components is not a trivial filtering, and advanced signal processing methods are needed to achieve the goal: to make the separate analysis of heart and respiration activities possible.

## 1.2. The bio-impedance signal decomposition

Assume that the EBI components are obtained from independent signal sources, thus the total signal  $S(t)$  can be expressed as a sum of the basic  $S_0$ , cardiac  $S_C(t)$  and respiratory  $S_R(t)$  components and unwanted artefacts, such as stochastic disturbances  $n_S(t)$  and motion artefact  $n_M(t)$  as well:

$$S(t) = S_0 + S_C(t) + S_R(t) + n_S(t) + n_M(t). \quad (1)$$

Since the expression (1) is only a single “view” to the electrical BI of the tissue region between the selected electrodes, the task can be described as

follows: we have five unknowns, which are needed to be found (separated), and only one known component – the sum of these unknown components, thus their linear combination.

Often the EBI signal can be expressed in a simplified form:

$$S(t) = S_C(t) + S_R(t). \quad (2)$$

After such simplification, through exclusion of some components other than cardiac and respiratory ones, the main problem remains – there are one known  $S(t)$  and two unknown ( $S_C(t)$  and  $S_R(t)$ ) components, interrelation of which can be described by a single expression. The latter two components have to be found using only the known observable variable  $S(t)$ .

Moreover, taking into account peculiarities of the cardiac and respiratory EBI components, we can list main difficulties, which have to be overcome:

- harmonic frequency domain spectra of the cardiac and respiratory components can often be overlapped;
- the decomposition procedure assumes that the separated components must remain unchanged individually;
- the EBI signal is non-stationary due to the variations of the heart rate and lung ventilation rate in time domain, and moreover, due to the motion artefacts, if such are presented in the EBI signal;
- low frequency nature of the cardiac and respiratory signal components.

An adaptive bio-impedance signal decomposer, intended to solve the signals separation task and to overcome related difficulties, was proposed by the author in [23–27].

The BISD is an on-line signal processing method, which decomposes the EBI signal into its components in time domain by continuously tracking the cardiac signal parameters, such as frequency (phase) and amplitude, and no external reference signals are needed.

### 1.3. Review of the bio-impedance signal decomposer

The BISD is a fast, in its reaction to the signal changes, method for separation of the cardiac and respiratory components. After applying enhancements, proposed in Section 2, the BISD produces now only one second constant delay of the separated cardiac and respiratory components with regard to the input EBI signal<sup>1</sup>. Moreover, the BISD uses only the total EBI as its input signal without need of any external reference signals.

Additionally, heart rate estimations, derived from other signals like ECG, can be used for supporting the procedure, if they are available, but this is certainly not obligatory. Such an approach eliminates the direct dependence on the ECG signal, but allows using additional data to increase the speed and reliability of the separation process.

---

<sup>1</sup> The previous version of the BISD produced two second delay.

First of all, the BISD is oriented to applications, requiring on-line, or even real-time, monitoring of both, the cardiac and respiratory activity.

### 1.3.1. The main structure of the BISD

The idea of the proposed solution is to replace  $S_C(t)$  and  $S_R(t)$ , expressed in Eq. (2), by their models  $S_{CM}(t)$  and  $S_{RM}(t)$ , respectively.

The conceptual block-diagram of the adaptive cardiac signal model based BISD, proposed in the previous publications and intended to separate the cardiac and respiratory EBI components, is shown in Fig. 1, where  $S(t)$  is the total input EBI signal;  $\tilde{S}_C(t)$  and  $\tilde{S}_R(t)$  are estimates of the cardiac and respiratory components, respectively and  $S_{CM}(t)$  and  $S_{RM}(t)$  are models of these signals; the functions  $f_{CM}(\tilde{S}_C(t))$  and  $f_{RM}(\tilde{S}_R(t))$  define the models of the cardiac and respiratory signals, respectively.

The block-diagram of the BISD practical realization is shown in Fig. 2. The module, which constructs the cardiac signal model by tracking its parameters synchronously with the estimated cardiac signal, is named signal-shape locked loop (SSLL), which is described in [25-27].

Since the respiratory EBI signal is much less deterministic than the cardiac one, the signal modelling procedure is more complicated. The BISD uses the FIR

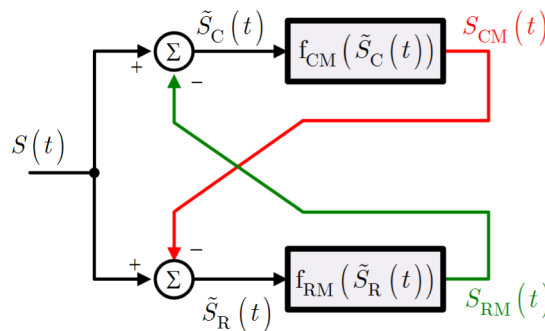


**Fig. 1.** The conceptual block-diagram of the bio-impedance signal decomposer into its cardiac and respiratory components.

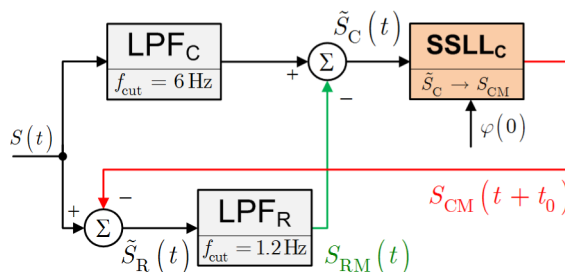


**Fig. 2.** The block-diagram of the bio-impedance signal decomposer.

(finite impulse response) low-pass-filter  $\text{LPF}_R$  with a constant cut-off frequency  $f_{\text{cut}} = 1.2 \text{ Hz}$  to suppress the remaining part of the cardiac EBI signal model  $S_{\text{CM}}(t)$ , subtracted from the input EBI signal  $S(t)$ . The second low-pass filter  $\text{LPF}_C$  is used in the upper branch of the BISD to compensate the delay of the respiratory signal in the  $\text{LPF}_R$ , and to suppress the high-frequency noise. Both filters,  $\text{LPF}_R$  and  $\text{LPF}_C$ , are linear phase FIR filters using Hamming window and are of the same length (in the last realization, both filters have lengths of 401 samples<sup>2</sup>). The latter peculiarity is needed to synchronize the outputs of the filters. Moreover, an additional time or phase shift ( $t_0$  or  $\varphi(0)$ , respectively) of the cardiac EBI signal model  $S_{\text{CM}}(t)$  towards the ‘future’ is required to compensate the delay of the signal in the filter  $\text{LPF}_C$  and synchronize the cardiac signal model  $S_{\text{CM}}(t)$  with the input EBI signal  $S(t)$ .

### 1.3.2. The cardiac EBI signal model

The real cardiac signal is a complicated waveform (Fig. 3, upper plot) and consequently several harmonic spectral components are needed to model this signal accurately (Fig. 3, lower plot).

Despite the fact that orthonormal basis (OB), formed from the harmonic functions,

$$\{H_k(t)\} = \{\cos_k(t), \sin_k(t)\}, \quad (3)$$

is powerful and widely used versatile signal processing tool, some application-specific orthonormal basis (ASOB) may give more appropriate and compact spectral representation of signals in practical situations.

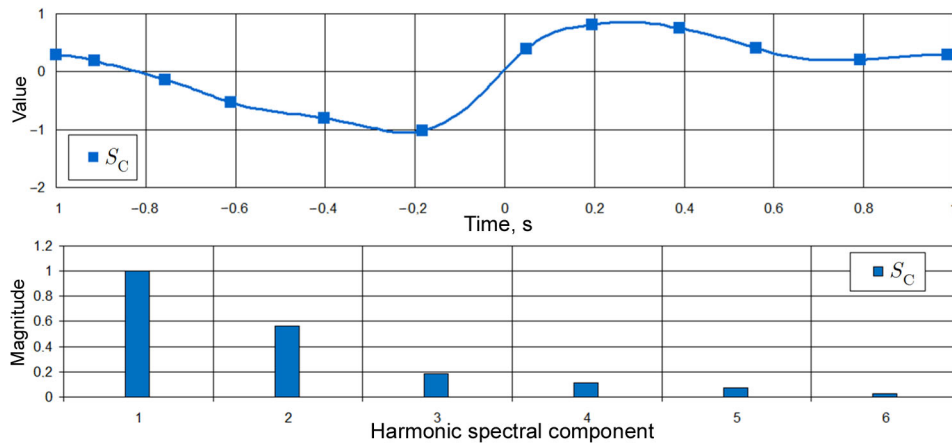


**Fig. 3.** An averaged through multiple periods and scaled cardiac EBI signal  $S_C(t)$  (upper plot); for illustration, scaled harmonic power spectrum of an averaged through multiple periods cardiac EBI signal is shown (lower plot).

<sup>2</sup> The clock frequency of the entire BISD is 200 Hz.

It is essential to use application-specific functions, representing characteristics of the signals to be processed. There are other conditions to be considered for flexibility and computational efficiency:

- using orthogonal system of functions makes possible independent detection of the components;
- as EBI signals are varying, the weighting function should have one or two parameters that could be used for adaptation to the waveform;
- simple integration formulas can be derived from orthogonal polynomials.

From classical orthogonal polynomials the proper choice would be Jacobi polynomials, which are defined in the interval  $[-1, 1)$  with the following weighting function

$$W^{A,B}(t) = (1-t)^A (1+t)^B, t \in [-1, 1). \quad (4)$$

Use of the Jacobi weight function for the cardiac signal modelling allows adapting the model shape to the signal shape by changing the values of parameters. Moreover, non-equal values of the parameters give non-symmetrical shape to the model. Such flexibility can be very useful for modelling the cardiac signal with a complicated shape.

The application-specific orthonormal basis has been designed applying the  $N$ th order Gram–Schmidt process, called also standard  $N$ th order Gram–Schmidt orthogonalization process.

Thus the result of this process is a set of orthogonal vectors  $Q_k(t)$ , where the in-phase component of the cardiac EBI signal model is constructed from the second  $Q_2(t)$  component of the proposed ASOB:

$$S_{CM}(t) = A_C(t) Q_2 \left( \frac{\varphi_C(t)}{\pi} \right), \quad (5)$$

where  $A_C$  is the detected amplitude and  $\varphi_C \in [-\pi, \pi)$  is the detected phase of the cardiac EBI component.

The first component  $Q_1(t)$  of the ASOB has to be orthogonal with the cardiac EBI signal, thus it can be used to synchronize the second component  $Q_2(t)$  of the ASOB against the cardiac signal  $S_C(t)$ .

In such a manner the model can approximate the most significant features of the one-period signal shape of the cardiac EBI signal.

The designed Jacobi weight function based ASOB is shown in Fig. 4, where one can see that the cardiac signal can be modelled much more accurately using only the second component of the ASOB, synchronous with the cardiac signal, than using the harmonic basis.

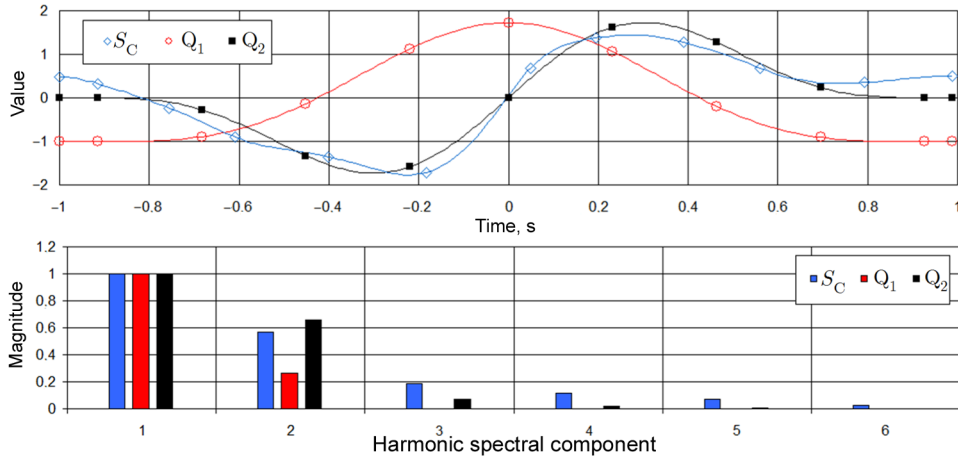


**Fig. 4.** The first and the second components of the designed ASOB and an averaged through multiples periods and scaled cardiac EBI signal  $S_C(t)$ , which is synchronous with the odd component  $Q_2(t)$  of ASOB (upper plot):  $A = B = 5$  (see Eq. (4)); scaled harmonic power spectra of the same signals (lower plot).

## 2. ENHANCEMENTS FOR THE BISD

In spite of the promising results of the BISD, a more accurate separation of the cardiac and respiratory components is required, even in extremely non-stationary conditions, such as an ambulatory one.

### 2.1. Semi-synchronous<sup>3</sup> amplitude and extrema estimator

An amplitude estimator, which was used in the BISD before applying the proposed one, is described in [23–27]. In that correlation-based estimator, the input cardiac signal is multiplied by the in-phase reference signal, after that an absolute value of the result is passed through the IIR low-pass filter for smoothing the final amplitude estimate and then scaling it by a predefined constant factor.

The main disadvantage of such estimator is sufficiently wide deviation of the multiplication result around its mean value. To effectively suppress these undesired deviations, the low-pass filter with a time constant larger than the period of the useful signal has to be used. However, this is not possible if we operate with such low frequency signals as the cardiac EBI signal, because in this case the estimator settling time is long and its reaction to the amplitude value changes becomes very slow. The slow reaction causes distortions in the BISD, because the input of the cardiac signal phase detector is divided by the estimated

<sup>3</sup> In this paper synchronous means synchronization with the cardiac EBI signal, if not defined otherwise.



amplitude value [24]. Moreover, the cardiac EBI signal model, in the BISD feedback, is multiplied by the same estimated value.

Next we describe the cardiac EBI signal amplitude estimator, which is based on the signal extrema searching algorithm. This algorithm operates synchronously with the cardiac EBI signal, if the BISD is locked in, and asynchronously in the opposite case. The algorithm is embedded into the block SSLLC in Fig. 2. The input signal for the proposed amplitude estimator is the separated cardiac signal  $\tilde{S}_C(t)$ .

### 2.1.1. The extrema looking algorithm

The proposed extrema looking algorithm can be logically divided into three stages. The first one is the continuously searching algorithm for extrema candidates. At this stage the algorithm compares the current signal value with the last maximum or minimum values respectively, as it is shown in the pseudo code below:

```
variables Maximum_New, Minimum_New /* extrema candidates values */
variable Input /* The input cardiac signal value */

IF Input > Maximum_New THEN
    SET Maximum_New TO Input
END IF

IF Input < Minimum_New THEN
    SET Minimum_New TO Input;
END IF
```

At the second stage, the found extrema values are applied to two median filters inputs.

If the BISD is not locked with the cardiac signal, then the median filter, intended for the maximum values, will get to its input the last found maximum value, at the moment when the cardiac signal model period starts or if the asynchronous time counter is equal to zero.

Similarly, the median filter, intended for the minimum values, will get to its input the last found minimum value, at the moment when the middle point of the cardiac signal model period is reached or if the asynchronous time counter is equal to zero as well.

In turn, the zero value will be assigned to the time counter three times per second. For more details the pseudo code is presented below:

```
variable Counter /* a milliseconds counter */
variables Max_Filter, Min_Filter /* Median filters4 for extrema candidates */

IF the BISD is locked THEN
    INCREMENT Counter;
```

---

<sup>4</sup> Median filters can be objects or functions, their realization is not discussed here.

```

IF Cardiac signal period begins OR Counter = 0 THEN
    APPLY Maximum_New AS input to Max_Filter;
    SET Maximum_New TO 0.0;
END IF

IF Cardiac signal period middle sample reached OR Counter = 0 THEN
    APPLY Minimum_New AS input to Min_Filter;
    SET Minimum_New TO 0.0;
END IF

IF Counter > 300ms THEN /* 3 times per second */
    SET Counter TO 0;
END IF

END IF

```

For the case when BISD is tracking the cardiac signal (is locked), the algorithm looks similar, but the input (cardiac) signal values will be applied to the median filters inputs at the moments when the cardiac signal model has its own minimum and maximum values, respectively. In this case, the time counter is keeping its value greater than zero. The pseudo code listing is the following:

```

variable Counter /* a milliseconds counter */
variables Max_Filter, Min_Filter /* Median filters for extrema candidates */
variable Input /* The input cardiac signal value */

IF the BISD is locked THEN
    SET Counter TO 1;

    IF Cardiac signal model at its maximum THEN
        APPLY Input AS input to Max_Filter;
        SET Maximum_New TO 0.0;
    END IF

    IF Cardiac signal model at its minimum THEN
        APPLY Input AS input to Min_Filter;
        SET Minimum_New TO 0.0;
    END IF

END IF

```

### 2.1.2. Estimating the amplitude value

The third stage is an estimation procedure of the cardiac signal amplitude value.

If the BISD is locked in, then the amplitude evaluation occurs at the cardiac signal period starting sample. In the opposite case it occurs also when the time counter (declared in the previous subsection) value will be equal to zero:

```

variable Amp /* the estimated cardiac signal amplitude value */
variable Swing /* the swing of the cardiac signal around its baseline */

IF Cardiac signal period begins OR Counter = 0 THEN
    COMPUTE Swing AS difference between median filters Max_Filter and
        Min_Filter outputs
    COMPUTE Amp AS Swing divided by 2
END IF

```

The both median filters, used in the proposed algorithm, have their lengths equal to five elements.

As a result, the estimated amplitude value is updated each time when the cardiac signal model period begins and is kept until the next period starts. In this case no multiplicative distortions occur during the cardiac signal period, if BISD is in the locked state.

### 2.1.3. Scaling the estimated amplitude

In the previous subsection the amplitude estimate was treated as maximum deviation of the signal from its base line. However, further it will be used in the meaning of a scaling factor and it must be normalized in the context of the selected signal basis

$$Amp\_Norm = \frac{Amp}{Amp\_Norm\_Factor\_I}. \quad (6)$$

Thus the input signal with the normalized amplitude, equal to unity, must exactly coincide with the synchronous component of the selected basis. And, consequently, for the basis described in Section 1.3.2, the normalization factor can be expressed as

$$Amp\_Norm\_Factor\_I = \max(Q_2(t)). \quad (7)$$

The proposed amplitude estimator noticeably improves the operation of the BISD, especially in the synchronization process speed and in more accurate and adequate continuous tracking capability of the signal amplitude. Also, updating the estimated amplitude values synchronously with the beginning of the input signal period, allows avoiding multiplicative distortions in the following signal processing steps. Results, which demonstrate these improvements, are presented in Section 3.

## 2.2. Lock-in detector

With an lock-in detector the situation is similar to the described above for the amplitude estimator. The well-known correlation-based lock-in detectors have

exactly the same disadvantages as the amplitude estimators of the same type (correlation-based) – the sufficiently wide deviation of the multiplication result around its mean value, which is difficult to suppress during reasonable time interval when operating with low-frequency signals such as the cardiac one.

Therefore we shall describe a lock-in detector, which is based on the normalized error level between the input signal and its synchronous model.

To increase robustness of the proposed detector, two kinds of error signals (differences) between the cardiac signal and its model are used. These are the continuous normalized error, described in Section 2.2.1, and its downsampled version (Section 2.2.2).

### 2.2.1. Cardiac signal model continuous error

Firstly, the input cardiac signal has to be normalized. The pseudocode of this procedure is:

```

variable Amp_Minimal /* the minimal allowed amplitude value */
variable Amp_Norm /* the normalized amplitude value from the section 2.1.2 */
variable Input /* The input cardiac signal value */

SET Amp_Minimal TO 0.05

IF Amp > Amp_Minimal THEN /* the condition to avoid division by 0 */

    DIVIDE Input BY Amp_Norm
    USE new value of Input

END IF

```

After that an error between the normalized input signal and its synchronous model  $Q_2(t)$  can be calculated and scaled by the factor  $Amp\_Norm\_Factor\_I$  (see Section 2.1.2):

$$Error = \frac{Input - Q_2(t)}{Amp\_Norm\_Factor\_I}. \quad (8)$$

And then the estimated error value is mapped into the range  $[0, 1]$  by using the normalized ( $a = 1$ ) Gaussian function with zero mean ( $\mu = 0$ ):

$$Gauss(x, \sigma, a, \mu) = a \exp\left(\frac{-(x - \mu)^2}{2\sigma^2}\right). \quad (9)$$

Thus the resulting mapped continuous error is:

$$Error\_Continuous = 1 - Gauss(Error, \sigma, a, \mu), \quad (10)$$

where  $a = 1$ ,  $\mu = 0$  and  $\sigma = 0.5$ .

To get the error value smoother in time domain, the continuous error is passed also through the first order Butterworth low-pass filter (cut-off frequency is 0.8 Hz).

### 2.2.2. Cardiac signal model downsampled error

The downsampled version of the error between the cardiac signal and its model is sampled at four points per cardiac signal model period. The points are placed near to the cardiac signal model extrema on the distances equal to  $\pm 0.1$  parts of the current period duration. Then the resampled error values are passed through a median filter of 5 points (downsampled points).

### 2.2.3. Lock-in detector summary

In the proposed lock-in detector an average of the continuous normalized error and its downsampled version is used. To compute the average, a zero order extrapolation procedure is applied to the downsampled error signal:

$$Error\_Avg = \frac{1}{2}(Error\_Continuous\_Smoothed + Error\_Downsampled). \quad (11)$$

After that the maximum value of the averaged error (11) is found during two cardiac signal model periods and is mapped into the range  $[0, 1]$ , using the normalized Gaussian function with zero mean:

$$Error\_Final = \text{Gauss}\left(\max_{\text{two card periods}}(Error\_Avg), 0.5, 1, 0.0\right). \quad (12)$$

To obtain two state logic output, the resulting error value (12) is passed through the trigger with hysteresis. The trigger is switching to high state at the threshold equal to 0.6 and to low state at the threshold equal to 0.42 (thresholds are selected empirically).

The proposed lock-in detector allows to determine, in different conditions, if the BISD is synchronized with the cardiac EBI signal or not. Results are presented in Section 3.

## 2.3. Conditioning the estimated cardiac signal frequency

Since the value of the time/phase shift of the cardiac signal model  $S_{CM}(t+t_0)$  (Fig. 2) depends on the freshly estimated cardiac signal frequency, and since this frequency can have unwanted variations during the cardiac signal period, then the accuracy of the entire BISD is reduced due to mismatches in time between the cardiac signal model and the cardiac component of the total input signal at the subtraction point (lower branch on the block diagram in Fig. 2).

To reduce such influence, the estimated frequency signal is sampled and held at the cardiac signal model extrema and at its zero crossing points.

### 3. RESULTS

The collection of bio-impedance EBI signals, recorded in clinical conditions, was used for testing the BISD. The impedance measurements were carried out by using the CircMon device (JR Medical Ltd, Estonia) and by using the bio-impedance measurement device designed in the Department of Electronics at Tallinn University of Technology.

Figures 5–7 present the time responses of the BISD to the input signals obtained from different persons. Each of the figures consists of five plots.

- The input signal  $S(t)$ , delayed by one second.
- The separated respiratory signal  $S_{RM}(t)$ .
- The separated cardiac EBI signal; the estimated maximum (red dotted line) and minimum (blue dotted line) levels and the amplitude (green dashed line with dots) are shown on the same plot.
- The lock-in detector output (solid black line) and  $Error\_Final$  signal (see Eq. (12)) value (blue dotted line).
- The estimated cardiac EBI signal frequency.

All signals on these figures are shown in relative units, obtained from the measuring devices, except the lock-in detector outputs and the cardiac signal frequency in Hz.

The input signal is scaled by the ramp-like function during the first 4 s to reduce the FIR filters transient artifacts and therefore to guarantee soft start of the BISD.

### 4. DISCUSSIONS AND CONCLUSIONS

Taking into account the possibility of the cardiac and respiratory components harmonic spectra overlapping and non-stationarity of these components, it seems to us that using time domain signal model based processing can be helpful in the defined task – to separate desired components, the cardiac and respiratory ones, from the total input EBI signal.

It became evident that at least the parametric time domain model of the cardiac component can be developed. The respiratory component is less deterministic due to its arbitrary and widely varying ventilation rate and therefore it is complicated to model it.

Moreover, the varying conditions, such as different patients with different kinds of pathologies require that the EBI signal decomposition method has to be as flexible as possible for successful operation. The method must be accurate and robust enough to be usefully implemented in clinical and especially in ambulatory conditions.

The amplitude estimator, lock-in detector and cardiac signal frequency conditioning, proposed in the paper, significantly improve the functionality of the BISD. Especially, enhancements are achieved in the reaction speed of the BISD

to the input EBI signal changes. From Figs 5 to 7 it is seen that after applying improvements to the BISD, it estimates cardiac signal amplitude during only few cardiac periods, even if very large difference between amplitudes exists in different conditions. And as a result, the entire BISD becomes locked during 8 s (including the 4 s soft start).

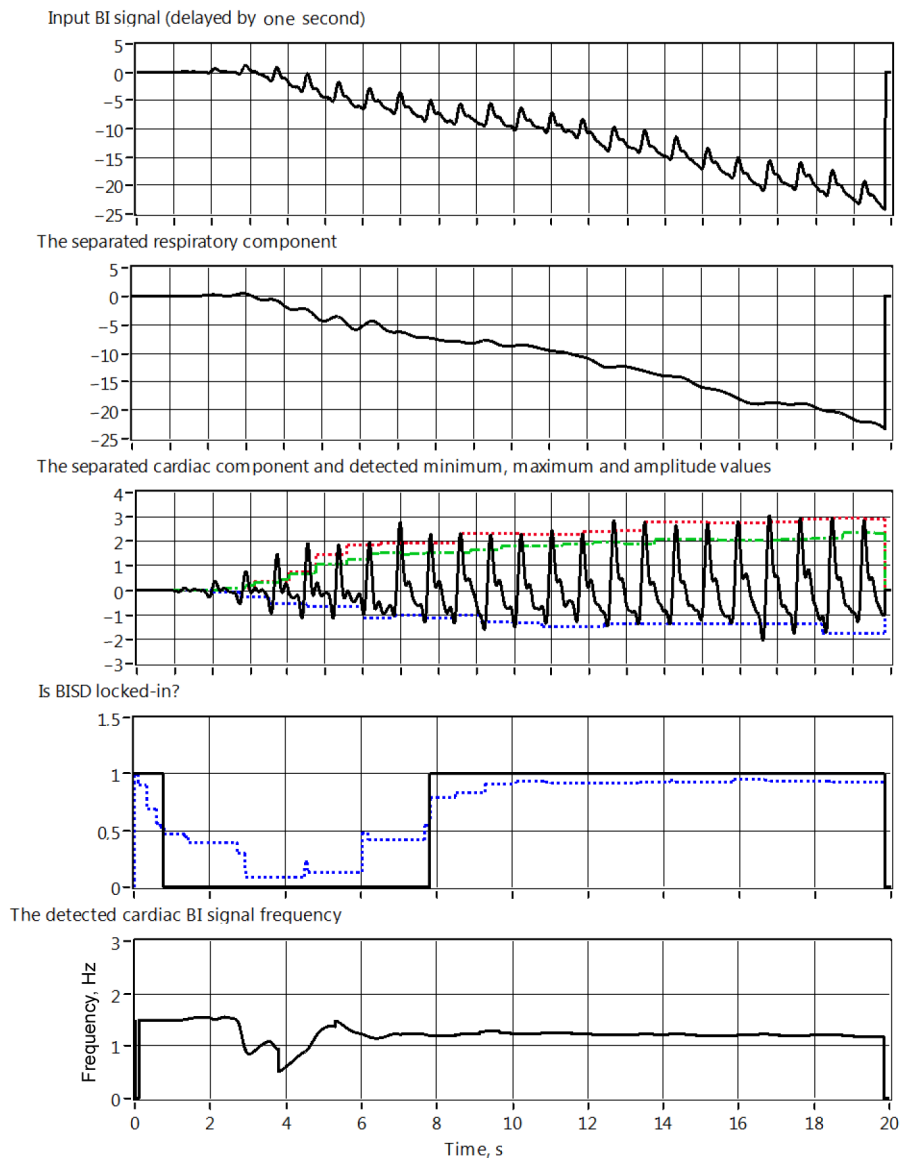


**Fig. 5.** The time domain response of the BISD with the proposed improvements used with the EBI signal, measured on the person No. 1.

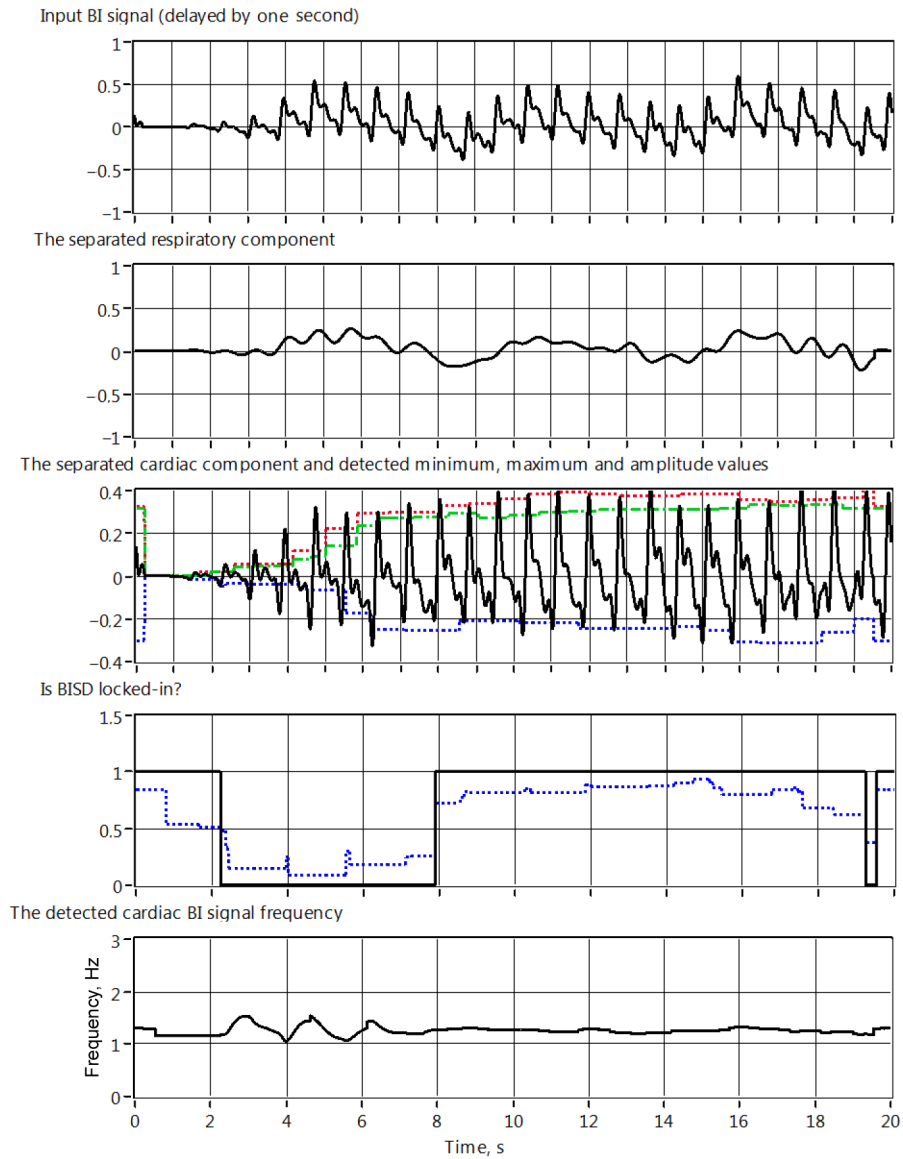


**Fig. 6.** The time domain response of the BISD with the proposed improvements used with the EBI signal, measured on the person No. 2.

The proposed improvements allowed to reduce the length of the FIR filters (Fig. 2) from 801 samples (in the previous version of the BISD [23–27]) to 401 samples. Thus the latency of the BISD is reduced from two to one second, taking into account that the whole BISD system sampling rate is 200 samples/s.



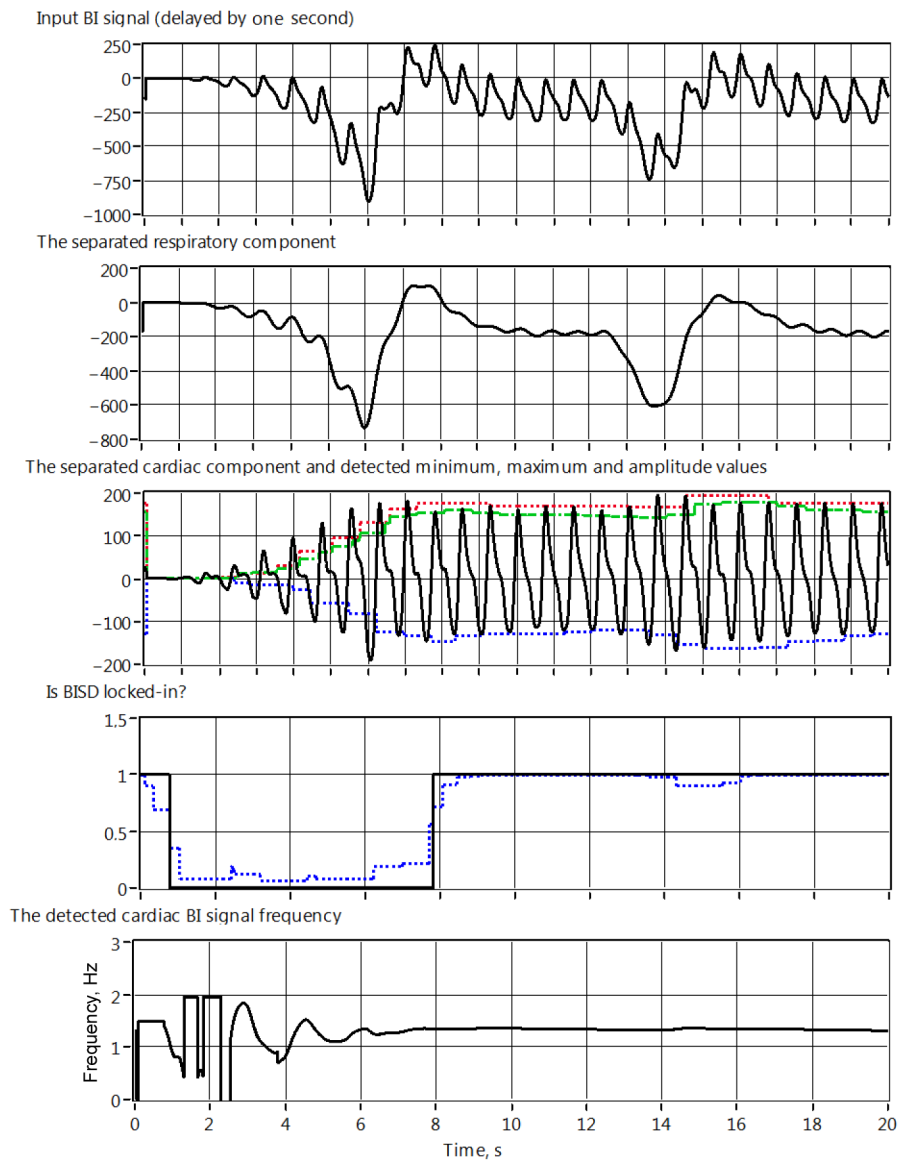


**Fig. 7.** The time domain response of the BISD with the proposed improvements used with the EBI signal, measured on the person No. 3.

## ACKNOWLEDGEMENTS

This work was supported by Target Financed Project SF0142737s06, Enterprise Estonia through the Competence Centre ELIKO, European Union through the European Regional Development Fund and the Centre of Research Excellence CEBE.

## REFERENCES

1. Atzler, E. and Lehmann, G. Über ein neues Verfahren zur Darstellung der Herz­­tätigkeit (Dielektrographie). *Arbeitsphysiol*, 1932, **6**, 636–680.
2. Nyboer, J., Bagno, S., Barnett, A. and Halsey, R. H. Radiocardiograms: electrical impedance changes in heart in relation to electrocardiograms and heart sounds. *J. Clin. Invest.*, 1940, **19**, 963.
3. Zlochiver, S., Freimark, D., Arad, M., Adunsky, A. and Abboud, S. Parametric EIT for monitoring cardiac stroke volume. *J. Physiol. Meas.*, 2006, **27**, S139–S146.
4. Newman, D. G. and Callister, R. The non-invasive assessment of stroke volume and cardiac output by impedance cardiography: a review. *Aviat. Space Environ. Med.*, 1999, **70**, 780–789.
5. Cotter, G., Schachner, A., Sasson, L., Dekel, D. and Moshkovitz, Y. Impedance cardiology revisited. *J. Physiol. Meas.*, 2006, **27**, 817–827.
6. Mond, H. L., Stratmore, N., Kertes, P., Hunt, D. and Baker, G. Rate responsive pacing using a minute ventilation sensor. *Pace*, 1988, **11**(suppl. II), 1866–1874.
7. West, J. B. *Respiratory Physiology: The Essentials*. Mir, Moscow, 1988 (in Russian).
8. Dell’Orto, S., Valli, P. and Greco, M. E. Sensors for rate adaptive pacing. *Indian Pacing and Electrophysiology J.*, 2004, **4**, 137–145.
9. Min, M., Parve, T. and Kink, A. Thoracic bioimpedance as a basis for pacing control. In *Electrical Bioimpedance Methods: Applications to Medicine and Biotechnology*. *Annals of the NY Acad. Sci.*, 1999, **873**, 155–166.
10. Webster, J. G. *Design of Cardiac Pacemakers*. IEEE Press, NJ, 1995.
11. Muzi, M., Jeutter, D. C. and Smith, J. J. Computer-automated impedance-derived cardiac indexes. *IEEE Trans. Biomed. Eng.*, 1986, **33**, 42–47.
12. Wang, X., Sun, H. H. and Van De Water, J. M. An advanced signal processing technique for impedance cardiography. *IEEE Trans. Biomed. Eng.*, 1995, **42**, 224–230.
13. Zhang, Y., Qu, M., Webster, J. G., Tompkins, W. J., Ward, B. A. and Bassett, D. R. Cardiac output monitoring by impedance cardiography during treadmill exercise. *IEEE Trans. Biomed. Eng.*, 1986, **33**, 1037–1042.
14. Woltjer, H. H., Bogaard, H. J. and M. de Vries, P. M. J. The intra- and interobserver variability of impedance cardiography in patients at rest and during exercise. *J. Physiol. Meas.*, 1996, **17**, 171–178.
15. Kim, D. W., Song, C. G. and Lee, M. H. A new ensemble averaging technique in impedance cardiography for estimation of stroke volume during treadmill exercise. *Frontiers Med. Biol. Eng.*, 1992, **4**, 179–188.
16. Hu, W., Sun, H. H. and Wang, X. A study on methods for impedance cardiography. In *Proc. 19th International Conference of the IEEE Engineering in Medicine and Biology Society, IEEE/EMBS 97*. Chicago, IL, USA, 1997, 2074–2077.
17. Yamamoto, Y., Mokushi, K., Tamura, S., Mutoh, Y., Miyashita, M. and Hamamoto, H. Design and implementation of a digital filter for beat-by-beat impedance cardiography. *IEEE Trans. Biomed. Eng.*, 1988, **35**, 1086–1090.
18. Chen, J. Z., Lin, Z. and McCallum, R. W. Cancellation of motion artefacts in electrogastrogram – a comparison of time-, transform- and frequency-domain adaptive filtering. In *Proc. IEEE SoutheastCon 1993*. Charlotte, NC, USA, 1993, 7.
19. Pandey, V. K. and Pandey, P. C. Cancellation of respiratory artifact in impedance cardiography. In *Proc. 27th Annual Conference on Engineering in Medicine and Biology*. Shanghai, China, 2005, 5503–5506.
20. Barros, A. K., Yoshizawa, M. and Yasuda, Y. Filtering noncorrelated noise in impedance cardiography. *IEEE Trans. Biomed. Eng.*, 1995, **42**, 324–327.
21. Ouyang, J., Gao, X. and Zhang, Y. Wavelet-based method for reducing respiratory interference in thoracic electrical bioimpedance. In *Proc. 20th Annual International Conference of IEEE Engineering in Medicine and Biology Society*, 1998, **20**, 1446–1449.

22. Pandey, V. K. and Pandey, P. C. Wavelet based cancellation of respiratory artifacts in impedance cardiography. In *Proc. 15th International Conference on Digital Signal Processing*. Cardiff, UK, 2007, 191–194.
23. Krivoshei, A. *Decomposition of the Electrical Bio-impedance Signal: A Signal Model Based Method for Separation of the Cardiac and Respiratory Components*. LAMBERT Acad. Publ., Saarbrücken, 2010.
24. Krivoshei, A., Min, M., Parve, T. and Ronk, A. An adaptive filtering system for separation of cardiac and respiratory components of bioimpedance signal. In *Proc. International Workshop on Medical Measurements and Applications*. Benevento, Italy, 2006, 10–15.
25. Krivoshei, A., Min, M. and Kukk, V. Signal-shape locked loop (SSLL) as an adaptive separator of cardiac and respiratory components of bio-impedance signal. In *Proc. International Workshop on Medical Measurements and Applications*. Warsaw, Poland, 2007, 47–52.
26. Krivoshei, A., Kukk, V. and Min, M. An adaptively tunable model of the cardiac signal for the bio-impedance signal decomposer (BISD). In *Proc. International Workshop on Medical Measurements and Applications*. Ottawa, Canada, 2008, 49–52.
27. Krivoshei, A., Kukk, V. and Min, M. Decomposition method of electrical bio-impedance signal into cardiac and respiratory components. *J. Physiol. Meas.*, 2008, **29**, S15–S25.

## **Parandatud täpsuse ja vähendatud latentsiga bioimpedantssignaali lahutaja**

Andrei Krivoshei

On vaadeldud mõõdetud elektrilise bioimpedantssignaali lahutamist südame-tegevusele ja hingamisele vastavateks komponentideks. Lahutamise raskus ja mittetriviaalsus on põhjustatud bioimpedantssignaali komponentide mittestatsionaarsusest ning nende spektrite ülekattuvusest. Ühe võimaliku probleemi lahendusena on antud ülevaade bioimpedantssignaali lahutajast (BISD). Koos BISD-süsteemiga on vaadeldud ka rakendusspetsiifilist, ortonormaalset baasi kasutavat mudelit südamesignaali kirjeldamiseks. Artikli põhiosas on südamesignaali amplituudi määramiseks esitatud poolsünkroonne hindamisalgoritm, mis baseerub kirjeldatud mudelil ja maksimumide otsimise algoritmil artikli samas osas. Eelnevale tuginevalt on välja töötatud südamesignaali *lock-in*-detektori ja saadud südamesignaali sageduse järeltöötamise algoritm. Kirjeldatud algoritmid võimaldavad BISD-süsteemi reaktsioonikiirust muutuvale sisendsignaalile parandada kuni kaks korda. Ka väga erinevate algsignaalide korral suudab BISD-süsteem anda adekvaatse hinnangu amplituudile ainult mõne südamelöögi järel. BISD-süsteem kohandub uuele signaalile umbes 8 sekundiga (kaasa arvatud 4-sekundiline “pehme start”). Pakutud täiustused lubavad BISD-süsteemi latentsust vähendada kahelt sekundilt ühele sekundile.